Korean J. Chem. Eng., **19**(3), 467-473 (2002)

Fabrication of Highly Ordered Pore Array in Anodic Aluminum Oxide

Sun-Kyu Hwang, Soo-Hwan Jeong, Hee-Young Hwang, Ok-Joo Lee and Kun-Hong Lee†

Department of Chemical Engineering, Electrical and Computer Engineering Division,
Pohang University of Science and Technology, San31, Hyoja-Dong, Nam-Ku, Pohang, Kyungbuk 790-784, Korea
(*Received 23 February 2001 • accepted 8 March 2002*)

Abstract−Highly ordered pore array in anodic aluminum oxide was fabricated by anodizing pure aluminum. The order of a pore array was affected by anodizing voltage, electrolyte temperature, and first anodizing time. A regular pore array with mean diameter of 24 nm and interpore distance of 109 nm could be formed by two-step anodization at 40 V, oxalic acid concentration of 0.3 M and electrolyte temperature of 15 °C. The measured interpore distance showed linearity with anodizing voltage. The diameter of pores was adjusted by pore widening treatment in a 5 wt% phosphoric acid solution at 30 °C after two step anodization. The mechanism of self-arrangement of pores could be explained by the repulsive interaction between the pore walls.

Key words: Anodic Aluminum Oxide, Self-Organization, Pore Array

INTRODUCTION

Nanoscale structures have recently attracted considerable scientific and commercial attention because of their unique electronic, magnetic, and optical properties. For example, nanochannel array can be applied to a recording medium to achieve recording densities of more than 16 Gbits/cm^2 [Horowitz et al., 1991; Nelson et al., 1998]. It can also be used for single-electron devices [Tager et al., 1997], and optoelectronic devices [Whitney et al., 1993].

Aluminum is always covered with a thin oxide film because of its high affinity for oxygen. Aluminum oxide film can also be produced when pure aluminum is used as an anode in an electrolytic cell. This oxide film is called anodic aluminum oxide (AAO) film. In this case, however, there form two types of oxide films, a dense barrier film and a porous film. Type of oxide film mainly depends on the nature of the electrolyte solution used in anodization. Barrier-type oxide film which is perfectly insoluble in the electrolyte solution is formed in neutral boric acid solution, ammonium borate or tartrate aqueous solutions (pH 5-7), ammonium tetraborate in ethylene glycol, and several organic electrolytes including citric, malic, and glycolic acids. Porous-type oxide film which is slightly soluble in electrolyte solutions is formed in sulfuric, phosphoric, chromic, and oxalic acids at almost any concentration. The thickness of barrier-type oxide film can only be controlled by anodizing voltage, whereas that of porous-type oxide film can be adjusted by the current density and anodizing time [Diggle et al., 1969].

Although porous AAO film has been commercially available for the last few decades, irregular arrangement of pores is obtained by conventional anodization technique. It is a rather recent development that a periodic pore arrangement in a porous AAO film can be obtained by two-step anodic oxidation method [Masuda et al., 1995]. After the first anodization is performed, the porous AAO layer is stripped out by an acid solution. Then the second anodization produces a highly-ordered, hexagonal close-packed pore array. This method is cheaper and easier than the electron beam lithography method to obtain a regular array of nano-sized pores. The pores have a uniform pore diameter in the range of 4-300 nm, high pore density in the range of 10^9-10^{11} cm^{-2} and an aspect-ratio of over 100 is easily obtained.

The formation of AAO film was affected by the anodic voltage, the temperature of electrolyte, and the first anodizing time [Li et al., 1998]. The anodic voltage and the temperature of electrolyte affect the growth rate of pores and the interpore distance. Also, first anodizing time has a significant effect on the ordering of pore arrays in AAO. The aim of this research is to study the effect of numerous parameters and to find the optimum condition for the formation of an AAO film with perfect hexagonal pore arrangement.

EXPERIMENTAL

A pure aluminum sheet (99.999%) of 1 mm thickness was degreased in acetone by ultrasonication. After ultrasonication, the specimens were rinsed several times in ethanol for more than 15 min, and finally rinsed in deionized water. The specimen was electropolished in a mixture of perchloric acid and ethanol ($HClO_4 : C_2H_5OH$=1 : 4 in volumetric ratio) to remove surface irregularities. The specimen was used as an anode while a flat Pt sheet or curved Al sheet was used as a cathode. The distance between the cathode and the anode was adjusted to be about 5 cm. A constant voltage of 20 V was applied between the cathode and the anode for 60-90 sec and the solution temperature was kept to be 7 °C during electropolishing. The electropolishing time was varied with the characteristics of the used Al specimens such as thickness and surface roughness. A constant voltage was applied by a computer-interfaced power supply (HOBANG, HBPS-1A200V). After electropolishing, the specimen was rinsed several times in ethanol for more than 15 min, then rinsed in deionized water and finally dried in an air stream. Next, the first-step anodization was carried out in a 0.3 M oxalic acid solution; the conditions for anodization such as temperature of electrolyte, anodizing voltage and first anodizing time were varied to find an optimum. Experimental setup was the same as what was used in

†To whom correspondence should be addressed.
E-mail: ce20047@postech.ac.kr

electropolishing, except that an oxalic acid was used instead of a perchloric acid-ethanol solution.

After the first anodization was completed, AAO layer was removed by immersing the specimen in a mixture of 1.8 wt% chromic acid and 6 wt% phosphoric acid at 65 °C for 1-4 hr. Finally, AAO film was obtained by the second anodization under the same condition as the first one. At all steps, the solution was stirred at a constant speed by a magnetic stirring bar. Electropolishing and anodizing were all carried out in a 500 mL or 1 L jacketed-beaker, which was designed to keep the temperature of the contained solution constant by using a refrigerated circulating bath (VWR Scientific Model 1157). The structure of AAO films was observed with Field Emission Scanning Electron Microscope (FE-SEM, Hitachis s-4200). The specimens were dried in a dessicator for at least an hour and then coated with Pt prior to SEM observation. For the examination of the cross-section of a bulk AAO film, the specimen was bent into V-shape to produce cracks parallel to the unbent edge of the specimen.

RESULTS AND DISCUSSIONS

An aluminum surface is usually flattened before anodization by an initial electropolishing step, which removes large surface irregularities. To obtain hexagonally ordered pore array in anodic oxide film, electropolishing is considered as an essential step. It was reported that ordered pore array could not be obtained with specimens prepared without electropolishing [Jessensky et al., 1998]. Fig. 1 shows the effect of electropolishing on the roughness of an aluminum specimen. Before electropolishing, the specimen exhibits surface roughness in m scale, but those large surface irregularities were removed after electropolishing. The specimen had mirror-like surface due to the surface roughness of a scale smaller than the wavelength of light. Electropolishing could be explained by the presence of a viscous layer, composed of an electrolyte, reaction products and dissolved metal ions [Aebersold et al., 1996]. Because viscous film thickness of the peak is thinner, the current density at the peak is higher than the current density at the valley. So the peaks are more quickly dissolved than valleys and the surface is smoothened due to the preferential attack on the peaks.

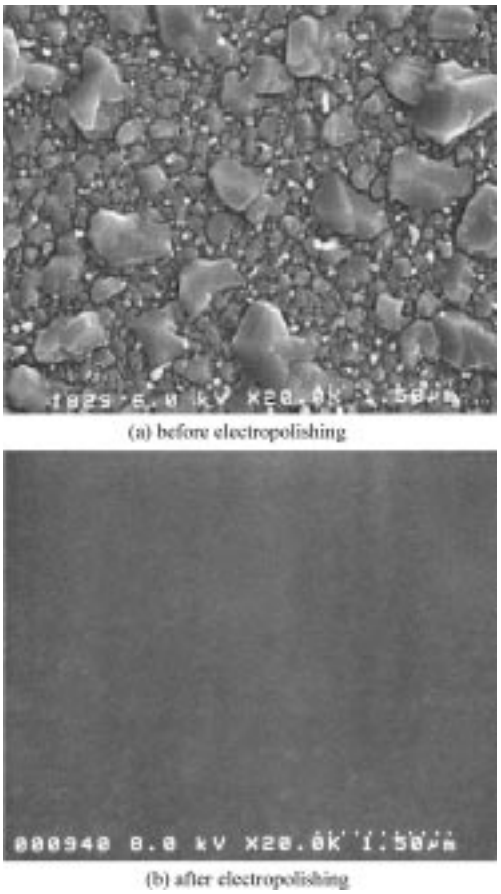

(a) before electropolishing

(b) after electropolishing

Fig. 1. Effect of electropolishing on the surface roughness. The specimen was electrochemically polished in a mixture of perchloric acid and ethanol ($HClO_4$: C_2H_5OH=1 : 4 in volumetric ratio). Applied DC voltage was 20 V between cathode and anode. The solution temperature was kept to be 7 °C.

Fig. 2 shows the SEM images of the top surfaces after anodization at various anodizing voltages and temperatures of electrolyte. The first and the second anodizing times were 12 hours and 20 min, respectively. The first anodization time mainly affects the pore arrangement, and the second anodization time only influences the pore length. The temperature of electrolyte was kept constant during each anodization. Fig. 2 clearly shows that the optimum condition for a perfect ordering of pores is 40 V at 15 °C for oxalic acid solution. The average pore diameter and the interpore distance are 24 nm and 109 nm, respectively. The domain size with perfect order was 3-4 μm and lattice mismatches were observed in a larger scale. Self-arrangement was observed even when the first anodization was carried out for only 2 hrs, but the ordered domain size was small. It was previously reported that the ordered domain size depends on the first anodization time and anodizing voltage [Li et al., 1998]. However, these effects are not so prominent. Although there is some ordering of pores at 40 V in 30 °C, they do not have a perfect hexagonal arrangement. At high voltages or high temperature, oxide dissolution rate at pore bottom may increase because the enhanced electrical field and current density shows large fluctuation. Therefore, local temperature may increase, so that stresses and rates of heat dissipation become nonuniform at pore bottom. Also, because the extent of volume expansion of aluminum oxide during anodization was larger, the pore arrangement might be disordered [Li et al., 1998]. At low voltages or low temperature, though anodization is very stable, the pore arrangements became very disordered. Because the repulsive interaction might become smaller, the expansion of volume during oxide formation at the Al/Al_2O_3 interface is smaller. However, regular pore array can be obtained if anodization is carried out for a long time.

The advantage of two-step anodization lies in the easy formation of a regular pore array. As the first anodization proceeds, the depth of pores increases and the arrangement becomes more regular. It was reported that the improvement of pore arrangement continued even after 60 hours of the first anodization [Shingubara et al., 1997]. The driving force for the self-arrangement of pores is thought to be the repulsive interaction between pores during pore growth. In the steady state pore growth period, oxide growth at the Al/Al_2O_3 interface and field-enhanced oxide dissolution at the Al_2O_3/electrolyte interface are in equilibrium. The repulsive interaction

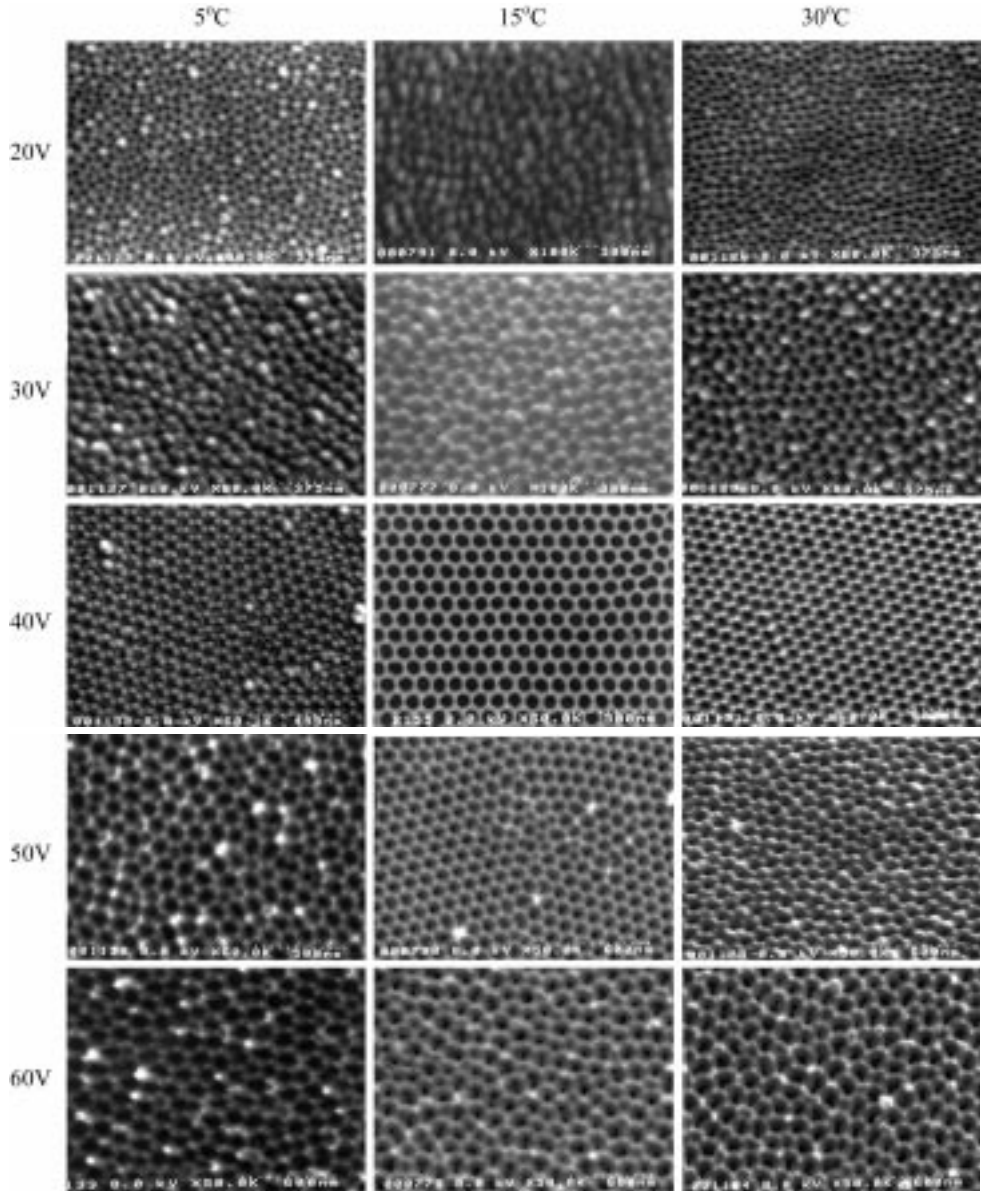

Fig. 2. Effect of anodizing conditions on the formation of pore arrays (top view). The anodizing solution was 0.3 M oxalic acid.

between neighboring pores results from mechanical stress due to the expansion of volume during oxide formation at the Al/Al_2O_3 interface. The oxide layer can freely expand only in the vertical direction while hexagonal close packing of pores occurs in the lateral direction to adjust the pores to a fixed volume [Jessensky et al., 1998]. It was reported that the best ordering of pore array was achieved for a moderate expansion factor of 1.4, i.e., the relative thickness of the porous AAO layer compared to the consumed aluminum. Table 1 summarizes the conditions for the formation of ordered pore arrays in AAO reported by previous investigators [Masuda et al., 1995, 1996, 1997, 1998; Al-Mawlawi et al., 1991; Li et al., 1998, 1999, 2000; Jessensky et al., 1998; Zhang et al., 1998]. These investigations only reported ordering conditions, but this study observed the various effects of anodizing parameters.

Because AAO film formed in the first anodization is nonordered at upper part of the AAO film, AAO film should be removed by wet chemical etching using a mixture of 1.8 wt% chromic acid and 6 wt% phosphoric acid. After AAO film was removed by wet chemical etching, the two-dimensional pattern of a regular array remained on the surface of the aluminum specimen. Fig. 3(a) shows the SEM image on the surface of an aluminum specimen after stripping of the AAO film formed by the first anodization for 12 hours. This figure clearly shows a hexagonal pattern on the surface of the aluminum specimen. Fig. 3(b)-(d) show the cross-sectional view of the AAO layer after second anodization. It is obvious that pore growth started from the surface of the aluminum specimen, and the pore growth progressed following this pattern in the second anodization.

The growth rate of pores (or equivalently, the etch rate of aluminum oxide layer) was a strong function of anodizing voltage and electrolyte temperature. Fig. 4 shows the voltage dependence of the growth rate at each temperature. The pore growth rate varied from 15 nm/min to 1 μm/min depending on anodizing voltage and temperature of electrolyte. The relationship between anodizing voltage and growth rate could be expressed by Eq. (1). This shows that

Table 1. Summary of previous investigations

Group	Ordering method	Pretreatment	Electrolyte	Temp. (°C)	Voltage (V)	Pore diameter	Ordered domain size
Al-Mawalawi et al.	No ordering	No	0.23 M Oxalic acid	25	11-20	n.a.	No ordering
Masuda et al.	Long anodization	No	0.3 M Oxalic acid	0	40	67±6	~2-3 μm
	2-step anodization	No	0.3 M Oxalic acid	17	40	50	n.a.
	Long anodization	No	0.3 M phosphoric acid	0	195	n.a.	>5 m
	Indentation	400 °C, 1 hr	0.3 M Oxalic acid	17	40	70	3 mm×3 mm
			0.3 M Oxalic acid	17	60	100	3 mm×3 mm
			0.04 M Oxalic acid	3	80	140	3 mm×3 mm
Li et al.	Long anodization	400 °C, 3 hr	0.3 M sulphuric acid	10	25	30	1-3 μm
			0.3 M Oxalic acid	1	40	70	1-3 μm
			10 wt% Phosphoric acid	3	160	250-300	1-3 μm
	2-step anodization	400 °C, 3 h	0.3 M Oxalic acid	5	40		1-5 μm
	2-step anodization	400 °C, 3 h	H_3PO_4 : CH_3O H : H_2O=1 : 10 : 89	−4	195	200	1-5 μm
	Pre-patterning by lithography	400 °C, 3 h	0.04 M Oxalic acid	5	85	120	
Jessensky et al.	Long anodization	500 °C, 3 h	0.3 M Oxalic acid	1	30-60 best 40	70	~μm size
			20 wt% Sulphuric acid		18-25 best 18.7	40	Smaller than that in oxalic acid
				1			
Zhang et al.	Modified 2-step anodization (3-step)	No	3% Oxalic acid	15	40	n.a.	4 μm
	2-step anodization	No	0.3 M Oxalic acid	15	40	n.a.	0.5-2 μm

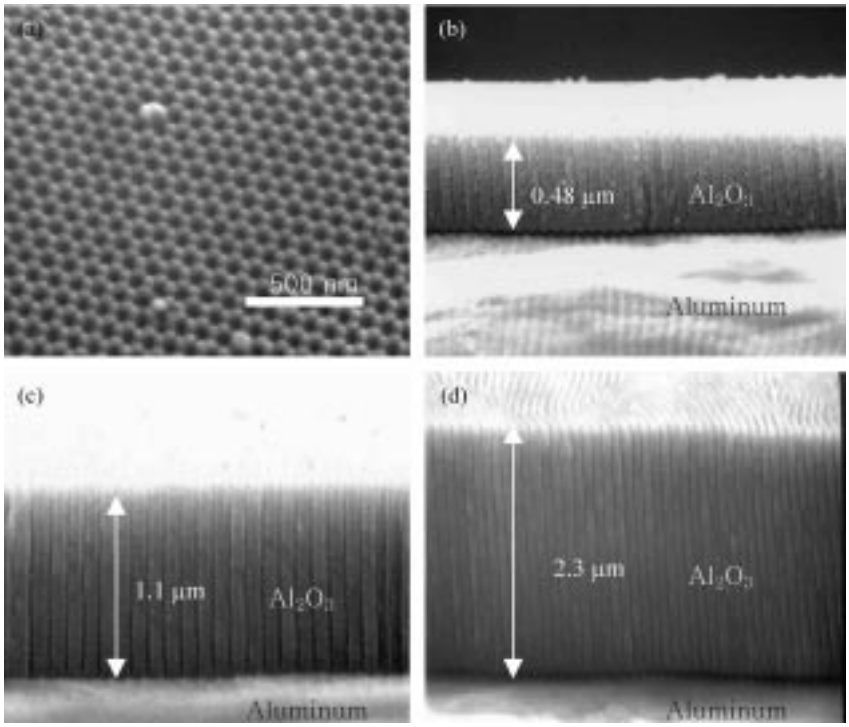

Fig. 3. Formation of regular pore arrays during anodization. (a) Hexagonal pattern on the surface of an aluminum specimen after stripping of the AAO layer formed by the first anodization (top view), (b) the AAO layer formed after the 2nd anodization for 5 min (side view); (c) for 10 min; (d) for 20 min.

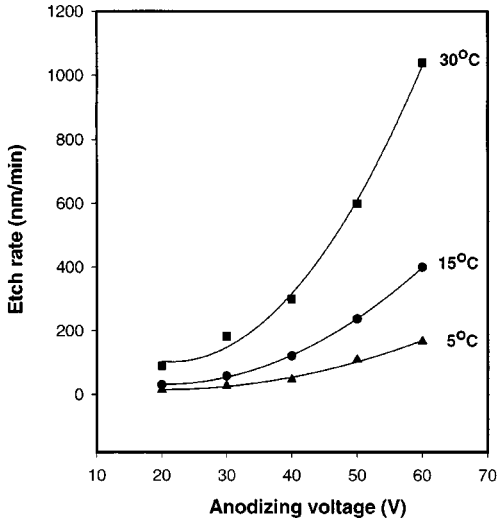

Fig. 4. Effect of anodizing voltage on the growth rate of pores. The anodizing solution was 0.3 M oxalic acid.

growth rate quadratically increases as anodizing voltage. Furthermore, growth rate of pores increases very rapidly with anodizing voltage at higher electrolyte temperature. It is thought that the pore growth rate increases due to either the field-enhanced dissolution or the temperature-enhanced dissolution.

$$R=51.33-3.71V_a+0.095V_a^2 \quad (30\ ^\circ C)$$
$$R=123.43-9.19V_a+0.230V_a^2 \quad (15\ ^\circ C)$$
$$R=392.30-26.92V_a+0.63V_a^2 \quad (5\ ^\circ C) \qquad (1)$$

The length of pores was proportional to the anodizing time. Here, extreme uniformity of the pore length should be pointed out. Fig. 5 shows the relationship between pore length and anodizing time. This linear relationship could be formulated to Eq. (2). Although the data was obtained at 15 °C and 40 V in 0.3 M oxalic acid, a linear relationship was always valid for other conditions. This linearity, however, could not be maintained when the anodization was carried out for more than several hours. It is thought that the diffusion of electrolyte solution to the bottom of the pores becomes the rate-determining step as the pore length increases.

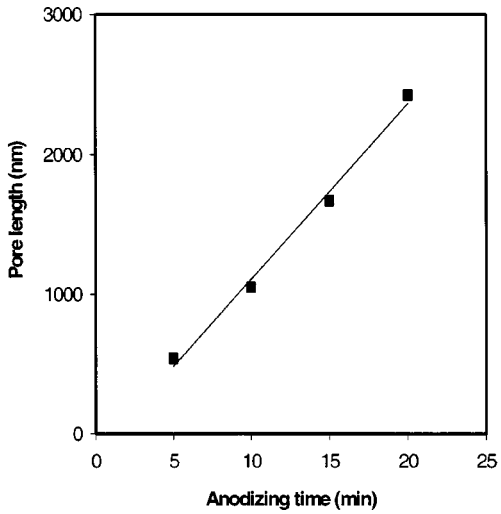

Fig. 5. Linear relationship between pore length and anodizing time. The anodization was carried out at 40 V in a 0.3 M oxalic acid solution at 15 °C. Pore length, l_p, shows linear relationship with anodizing time, t_a: $l_p=-147.75+125.53t_a$.

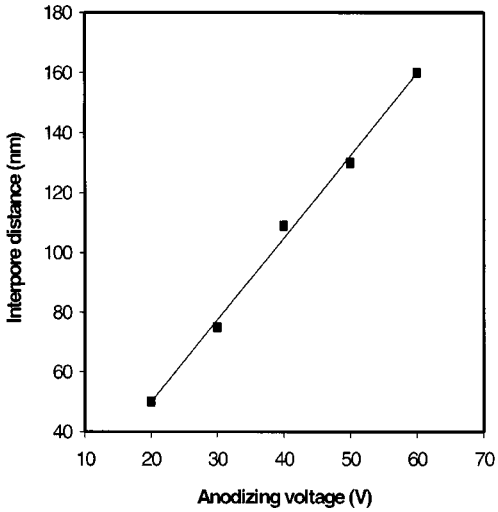

Fig. 6. Voltage dependence of interpore distance. The anodization was carried out under voltage ranges of 20-60 V. The measured interpore distance, D_i showed linearity with anodizing voltage, V_a: $D_i=-5.2+2.75V_a$.

$$l_p=-147.75+125.53t_a \qquad (2)$$

Voltage dependence of interpore distance is shown in Fig. 6. Interpore distance was determined as the average of the interpore distances obtained from SEM images. The specimens anodized under voltage ranges of 20-60 V show pore distances in the range of 50-160 nm. The measured interpore distance shows linearity with anodizing voltage. The relationship could be expressed by Eq. (3). One interesting observation is that interpore distance only depends upon anodizing voltage, not upon the temperature of electrolyte. This result corresponds to the earlier report [Li et al., 1999].

$$D_i=-5.2+2.75V_a \qquad (3)$$

It is possible to control the pore diameter without any change in pore density: it is frequently referred as pore widening. Pore widening results from the dissolution of aluminum oxide in the pore wall in an acidic solution. Fig. 7(a) shows the effect of widening time on the diameter of pores. This particular sample was prepared by the two-step anodization at 40 V in a 0.3 M oxalic acid solution at 15 °C, and widening was performed in a 0.1 M phosphoric acid at 30 °C. The mean pore diameter was 24 nm before pore widening treatment and widened to 74 nm after 50 min of pore widening. A quadratic relationship was obtained between the pore diameter and widening time, which could be reduced to Eq. (4).

$$D_p=24.703-0.116t_w+0.0221t_w^2 \qquad (4)$$

This results agrees with the earlier reports [Al-Mawlawi et al., 1991, 1994]. Fig. 7(b) and (c) show cross-sectional view of AAO before and after widening treatment for 50 min at 30 °C, respectively. They clearly demonstrate the increase of pore diameter. Pore widening treatment is accompanied with the thinning of the barrier

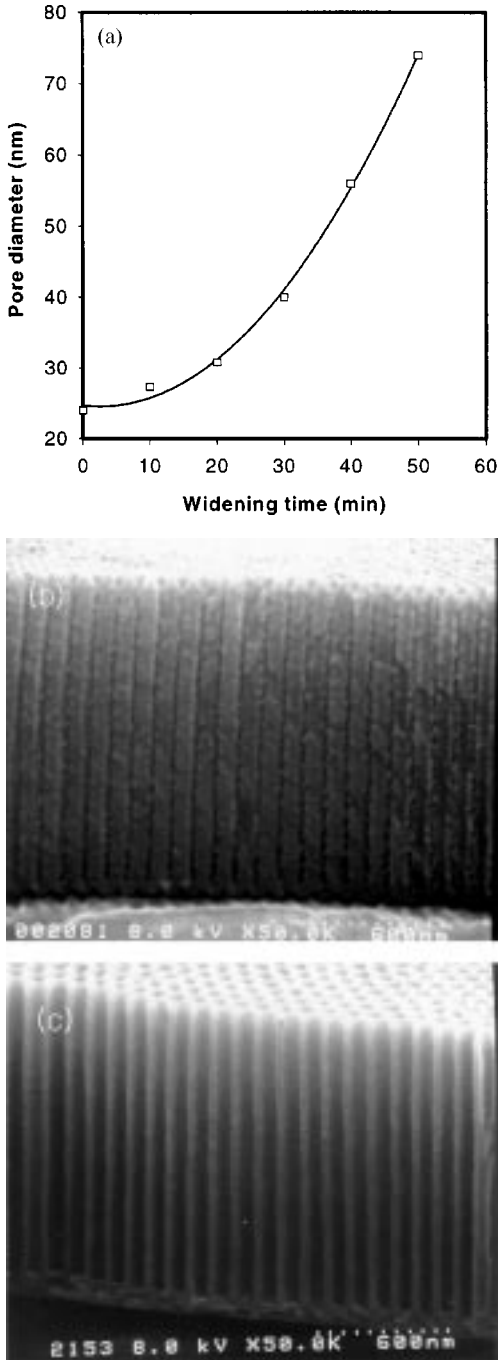

Fig. 7. Dependence of pore diameter upon widening time. Anodization was carried out at 40 V in a 0.3 M oxalic acid solution at 15 °C and widening was performed in a 0.1 M phosphoric acid, 30 °C. (a) Dependence of pore diameter (D_p) upon widening time (t_w); (b) cross-sectional view of AAO before widening treatment, (c) after widening treatment for 50 min at 30 °C.

layer. Barrier layer thinning is essential for the electroplating of a metal at the pore bottom of AAO film because electrons can tunnel easily through a thinner barrier layer. Barrier layer can be completely removed to make a membrane. Complete removal of barrier layer can be realized by lowering the anodizing voltage in a small step [Sui et al., 2001].

There is every possibility that the inter-pore dimension in an AAO template can be controlled by the combination of the method shown in this work with the indentation method [Masuda et al., 1997]. A pretextured pattern on the surface of an aluminum specimen can be made by nano-indentation using a mold with a desired inter-pore dimension of convexes. The obtained concaves of the aluminum surface act as a pilot holes in the initial pore development during anodization. If anodization is performed the voltage which produces the same pore dimension with the mold, AAO template with desired dimension can be made. An ordered AAO template with various pore dimensions and diameters can be obtained with additional pore widening treatment.

CONCLUSIONS

Ordered pore array of nanometer scale can be obtained by anodizing pure aluminum specimen in acidic solutions. The order of pore array is affected by anodizing voltage, electrolyte temperature, and the first anodizing time. The window for the perfect hexagonal array is rather narrow. In a 0.3 M oxalic acid solution, a highly ordered structure with pore diameter of 24 nm and interpore distance of 109 nm was obtained by two-step anodization at 40 V in 15 °C. The growth rate of pores was affected by anodizing voltage and the temperature of electrolyte. The interpore diameter linearly increased with anodizing voltage. The diameter of pores could be adjusted between 24 nm and 74nm without any change in pore density by pore widening treatment in a 0.1 M phosphoric acid solution at 30 °C after two-step anodization. These results could be used for making ordered AAO template with various pore dimensions and diameters.

These nanotemplates can be applied to the various fields, such as filtration, duplication matrixes, evaporation masks, the high-density recording media, rechargeable batteries [Mazalev et al., 2001], optoelectronic devices and template for the growth of metal or semiconductor nanowire [Routkevitch et al., 1996]. Also it might be obtained the ordered nanotemplate with desired pore dimension by using pre-textured aluminum and suitable anodizing voltage.

ACKNOWLEDGEMENT

The authors would like to thank the Ministry of Education of Korea for its financial support toward the Electrical and Computer Engineering Division at POSTECH through its BK21 program.

NOMENCLATURE

l_p : pore length [nm]
t_a : anodizing time [min]
V_a : anodizing voltage [V]
R : growth rate [nm/min]
D_i : interpore distance [nm]
D_p : pore diameter [nm]
t_w : pore widening time [min]

REFERENCES

Aebersold, J. F., Stadelmann, P. A. and Matlosz, M., "A Rotating Disk-

Electropolishing Technique for TEM Sample Preparation," *Ultramicroscopy*, **62**, 157 (1996).

Al-Mawlawi, D., Coombs, N. and Moskovits, M., "Magnetic Properties of Fe Deposited into Anodic Aluminum Oxide Pores as a Function of Particle Size," *J. Appl. Phys*., **70**, 979 (1991).

Al-Mawlawi, D., Liu, C. Z. and Moskovits, M., "Nanowires Formed in Anodic Oxide Nanotemplates," *J. Mater. Res.*, **9**, 1014 (1994).

Diggle, J. W., Downie, T. C. and Goulding, C. W., "Anodic Oxide Films on Aluminum," *Chem. Rev.*, **69**, 365 (1969).

Horowitz, G., Fichou, D., Peng, X. and Garnier, F., "Thin-Film Transistors Based on Alpha-Conjugated Oligomers," *Synth. Met.*, **41-43**, 1127 (1991).

Jessensky, O., Müller, F. and Gösele, U., "Self-Organized Formation of Hexagonal Pore Arrays in Anodic Alumina," *Appl. Phys. Lett.*, **72**, 1173 (1998).

Jessensky, O., Müller, F. and Gösele, U., "Self-Organized Formation of Hexagonal Pore Structures in Anodic Alumina," *J. Electrochem. Soc.*, **145**, 3735 (1998).

Li, A. P., Müller, F. and Gösele, U., "Polycrystalline and Monocrystalline Pore Arrays with Large Interpore Distance in Anodic Alumina," *Electrochem. Solid-State Lett*., **3**, 131 (2000).

Li, A. P., Müller, F., Birner, A., Nielsch, K. and Gösele, U., "Fabrication and Microstructuring of Hexagonally Ordered Two-Dimensional Nanopore Arrays in Anodic Alumina," *Adv. Mater*., **11**, 483 (1999).

Li, A. P., Müller, F., Birner, A., Nielsch, K. and Gösele, U., "Hexagonal Pore Arrays with a 50-420 nm Interpore Distance Formed by Self-Organization in Anodic Alumina," *J. Appl. Phys*., **84**, 6023 (1998).

Li, F., Zhang, L. and Metzger, R. M., "On the Growth of Highly Ordered Pores in Anodized Aluminum Oxide," *Chem. Mater.*, **10**, 2470 (1998).

Masuda, H. and Fukuda, K., "Ordered Metal Nanohole Arrays Made by a Two-step Replication of Honeycomb Structures of Anodic Alumina," *Science*, **268**, 1466 (1995).

Masuda, H. and Satoh, M., "Fabrication of Gold Nanodot Array Using Anodic Porous Alumina as an Evaporation Mask," *Jpn. J. Appl. Phys*., **35**, L126 (1996).

Masuda, H., Yada, K. and Osaka, A., "Self-Ordering of Cell Configuration of Anodic Porous Alumina with Large-Size Pores in Phosphoric Acid Solution," *Jpn. J. Appl. Phys*., **37**, L1340 (1998).

Masuda, H., Yamada, H., Satoh, M., Asoh, H., Nakao, M. and Tamamura, T., "Highly Ordered Nanochannel-Array Architecture in Anodic Alumina," *Appl Phys. Lett*., **71**, 2770 (1997).

Mazalev, A., Magaino, S. and Imai, H., "The Formation of Nanoporous Membranes from Anodically Oxidized Aluminum and Their Application to Li Rechargeable Batteries," *Electrochim. Acta*, **46**, 2825 (2001).

Nelson, S. F., Lin, Y.-Y., Gundlach, D. J. and Jackson, T. N., "Temperature-Independent Transport in High Mobility Pentacene Transistors," *Appl. Phys. Lett*., **72**, 1854 (1998).

Routkevitch, D., Tager, A. A., Haruyama, J., Almawlawi, D., Moskovits, M. and Xu, J. M., "Nonlithographic Nano-wire Arrays: Fabrication, Physics, and Device Applications," *IEEE Trans. Electron Devices*, **43**, 1646 (1996).

Shingubara, S., Okino, O., Sayama, Y., Sakaue, H. and Takahagi, T., "Ordered Two-Dimensional Nanowire Array Formation Using Self-Organized Nanoholes of Anodically Aluminum," *Jpn. J. Appl. Phys*., **36**, 7791 (1997).

Sui, Y. C., Acosta, D. R., González-León, J. A., Bermúdez, A., Feuchtwanger, J., Cui, B. Z., Flores, J. O. and Saniger, J. M., "Structure, Thermal Stability, and Deformation of Multibranched Carbon Nanotubes Synthesized by CVD in the AAO Template," *J. Phys. Chem. B*, **105**, 1523(2001)

Tager, A. A., Xu, J. M. and Moskovits, M., "Spontaneous Charge Polarization in Single-Electron Tunneling Through Coupled Nanowires," *Phys. Rev. B*., **55**, 4530 (1997).

Whitney, T. W., Jiang, J. S., Searson, P. C. and Chien, C. L., "Fabrication and Magnetic Properties of Arrays of Metallic Nanowires," *Science*, **261**, 1316 (1993).

Zhang, L., Cho, H. S., Li, F., Metzger, R. M. and Doyle, W. D., "Cellular Growth of Highly Ordered Porous Anodic Films on Aluminum," *J. Mater. Sci. Lett.*, **17**, 291 (1998).